

(1). Since the effective-mass description is as amenable to numerical calculations as conventional energy-dependent local descriptions, it is to be hoped it will be employed in the future in the analysis of scattering data. This is particularly incumbent where the parameters of such potentials are to be analyzed for nuclear structure information, such as nuclear mass radii. In addition, within this framework the nonlocal effects can be transparently introduced into, for instance, distorted-wave Born-approximation calculations¹¹ and reaction formulas, and in a manner which is consistent with flux conservation. As we see it, if an optical description is in fact applicable to a problem, the residual nonlocal effects should generally be accountable through the procedures outlined here.

The author is indebted to Dr. J. P. Svenne for his interest and direct assistance. The author also acknowledges helpful conversations with

Dr. W. Falk, Dr. B. S. Bhakar, Dr. J. M. Nelson, Dr. W. T. H. van Oers, and Professor E. W. Vogt.

¹F. Perey and B. Buck, Nucl. Phys. **32**, 353 (1962).

²F. G. Perey, in *Direct Interactions and Nuclear Reaction Mechanisms*, edited by E. Clementel and C. Villi (Gordon and Breach, New York, 1963), p. 125.

³N. Austern, Phys. Rev. **137**, B752 (1965).

⁴F. G. Perey, Phys. Rev. **131**, 745 (1963).

⁵F. G. Perey and D. S. Saxon, Phys. Lett. **10**, 107 (1964).

⁶G. W. Greenlees, G. J. Pyle, and Y. C. Tang, Phys. Rev. Lett. **17**, 33 (1966).

⁷G. W. Greenlees, G. J. Pyle, and Y. C. Tang, Phys. Rev. **171**, 1115 (1968).

⁸W. T. H. van Oers, to be published.

⁹L. Kisslinger, Phys. Rev. **98**, 761 (1955).

¹⁰T. E. O. Ericson and M. Ericson, Ann. Phys. (New York) **36**, 323 (1966).

¹¹J. M. Nelson and B. E. F. Macefield, Oxford Nuclear Physics Laboratory Report No. 18/69 (unpublished).

Electron Scattering from Aligned and Nonaligned Ho¹⁶⁵ Nuclei*

F. J. Uhrhane, J. S. McCarthy,† and M. R. Yearian

High Energy Physics Laboratory, Stanford University, Stanford, California 94305

(Received 14 January 1971)

The differential scattering cross sections have been measured for electron scattering from randomly oriented and aligned Ho¹⁶⁵ nuclei. The alignment axis was parallel to the direction of the momentum transferred to the nucleus. Incident electron energies from 160.6 to 462.2 MeV were used at a fixed polar scattering angle of 36°. Available theories are unable to explain the measured difference between the aligned and nonaligned cross sections.

The charge distributions of many nuclei have been investigated at Stanford University in recent years.¹ The method of fast-electron scattering has been developed to the point where even such small effects as are caused by oscillatory shell structure can be examined.² This technique is especially facilitated in the case of spherically symmetric nuclei, whose differential cross sections show strong diffraction structure. Nuclei with a large deformation, however, do not exhibit such well-defined diffraction, and a determination of their nuclear-charge parameters is considerably more difficult.³ The reduced diffraction effect is believed to be caused in part by the random orientation of the deformed nucleus. The effective nuclear "radius" as measured by electron scattering is a function of the relative orientation of the incident electron and the axis of the nucleus.

Safrata and McCarthy constructed the first cryostat to orient nuclei successfully for electron scattering. The first experiment to measure cross sections for an oriented nucleus⁴ was performed (in 1966) in order to obtain information about nuclear deformity. In the experiment the Stanford Mark III linear accelerator was used to scatter electrons from a target of Ho¹⁶⁵ in which the major axis of the prolate nucleus was oriented perpendicular to the scattering plane. This Letter reports a second experiment in which the major axis was oriented in the scattering plane and parallel to the momentum transferred to the nucleus by the scattered electrons.

Ho¹⁶⁵ has a large intrinsic quadrupole moment^{5,6} of about $(7.6 \pm 1.5) \times 10^{-24}$ cm². Holmium metal has an antiferromagnetic helical structure below 20°K.⁷ By application of a magnetic field in the basal plane perpendicular to the axis of hexagonal

symmetry it is possible to form a ferromagnetic structure. Our target was in the shape of a thin plate, 0.85 mm thick, and was cut from a single crystal in such a way that the direction of easy magnetization was in the plane of the plate.

It is known from low-temperature specific-heat measurements on holmium metal⁸ that, due to unpaired 4*f* electrons, there is an effective magnetic field of 9.3 MG acting at the site of the nucleus. This strong magnetic field enables one to achieve a high degree of nuclear orientation at the temperatures of liquid He³. The basic cryostat has been described in Ref. 4. For this experiment it was necessary to modify the cryostat to allow for an iron C-type magnet which provided a field of about 4.6 kG in the proper direction at the target site. 94% of saturation magnetization was achieved in the single-crystal target, and 26% in a polycrystalline target used for comparison purposes.

The target samples were mounted in a finned copper frame, and both the targets and the frame were submerged in liquid He³. The temperature of the liquid was determined by monitoring its vapor pressure. The temperature distribution of the Ho samples was calculated using the equation $\nabla \cdot (K\nabla T) - q = 0$, where *K* is the thermal conductivity of Ho metal and *q* is the sum of the heat-source and -sink distributions in it. We used $K = 2.85T$ in mW/cm °K, which is valid for temperatures below 1.0°K.⁹ The term *q* is com-

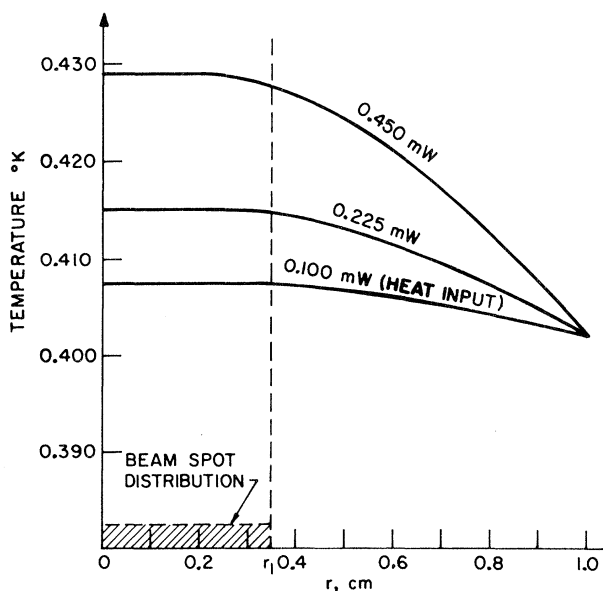


FIG. 1. Temperature distribution in the Ho single crystal as a function of radius from the beam-spot center. A bath temperature of 0.402°K is assumed for the calculation.

posed of heating gained as a result of ionization by the incident electron beam,¹⁰ and of heat lost from the crystal surface directly to the surrounding liquid. The Kapitza resistance was taken to be $R_K = 0.067T^{-3}$ mW⁻¹ cm² °K for the calculation. The resulting temperature distribution for several beam intensities is shown in Fig. 1. The beam intensity used was 1.9×10^{-5} μA, giving a heat input of 0.22 mW and a sample temperature in the beam spot of 0.415 ± 0.015 °K. The alignment in the single crystal was approximately 44% of the theoretical maximum under these conditions, and the alignment of the polycrystalline target was less than 10%.

The experiment was done at a polar scattering angle of 36° and at incident energies from 160.6 to 462.2 MeV (see inset, Fig. 2). The scattered electrons were detected by a 100-channel scintillation ladder¹¹ located in the image plane of a 72-in. double-focusing iron spectrometer.¹²

The trajectories of the incident electron beam and scattered electrons in the aligning field were not exactly calculable. It was necessary to determine these trajectories experimentally in order to measure the actual angles at which the data were taken. The alignment axis was horizontal and generally across the beam line, and a field

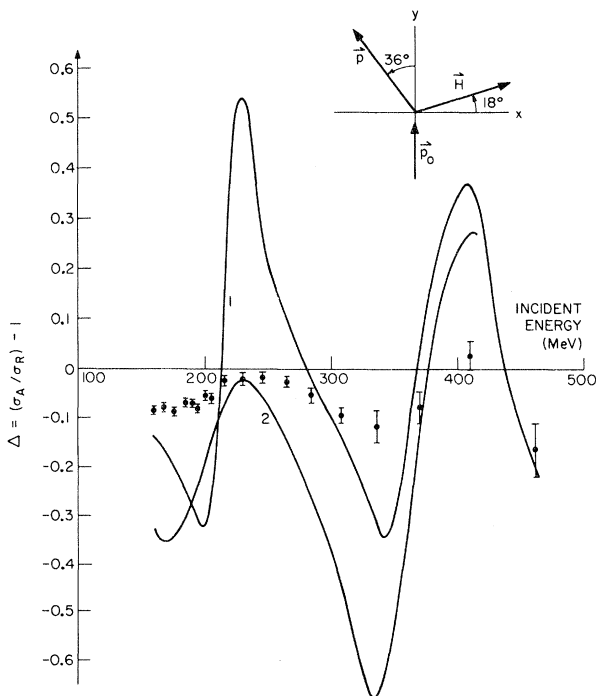


FIG. 2. Comparison of the experimental quantity Δ with Greenstein-Born approximation (curve 1) and with a calculation by Wright (curve 2). Data were taken at a polar scattering angle of 36°.

in this direction bent the beam up or down depending upon the polarity of the magnet. Similarly the scattered electrons were deflected, resulting in a tipping of the scattering plane. The changes in the polar and aximuthal scattering angles due to deflection in the field were measured on an apparatus using the floating wire method.¹³ The adjustments necessary to maintain the spectrometer at a true polar angle of 36° were computed; however it was not possible to maintain the azimuthal angle at 0° . The azimuthal angle monotonically varied from 5° to 15° as the incident energy varied from 462.2 to 160.6 MeV.

The comparison sample of polycrystalline Ho was frequently alternated with the single crystal. This procedure reduced the effects of various fluctuations and drifts in the accelerator and counting system. The observed change in cross section between aligned and nonaligned Ho¹⁶⁵ was calculated from the ratio of the data obtained from the two target samples, taking into consideration the actual alignment present in both samples.

The collective nuclear model of Bohr and Mottelson¹⁴ for a highly deformed nucleus such as Ho¹⁶⁵ predicts low-lying excited states which correspond to a collective rotation of the outer nucleons. These levels are excited in Ho¹⁶⁵ with energies less than 0.3 MeV.¹⁵ The momentum resolution of the detecting system did not allow a separation to be made between the inelastically scattered electrons, which excited these states, and the elastically scattered electrons. The experimental and theoretical cross sections presented will therefore include contributions from both elastic and inelastic scattering.

The cross sections were found in the usual way by measuring the area under the elastic (plus inelastic) peak after counting-rate corrections and radiative corrections¹⁶ were applied. Theoretical cross sections were computed by Wright¹⁷ assuming a Bohr-Mottelson representation of the nucleus. The nuclear charge distribution was assumed to consist of a spherical-plus-quadrupole term. The spherical component was treated using a phase-shift analysis while the quadrupole interaction was approximated to first order using the distorted-wave method for electrons. A Fermi distribution was used for the spherical charge distribution, with $\rho_0(r) = \{1 + \exp[(r - C_0)/z_1]\}^{-1}$, where $C_0 = 6.12$ fm and $z_1 = 0.57$ fm. The quadrupole charge was taken to be $\alpha r(d\rho_0/dr) \times P_2(\cos\gamma)$, where γ was the angle between the

symmetry axis of the nucleus and the alignment axis, and α was chosen to set the intrinsic quadrupole moment to 8×10^{-24} cm².

To illustrate the effect of alignment on the cross sections, we define $\Delta = \sigma_A/\sigma_R - 1$, where σ_A and σ_R are the cross sections for aligned and randomly oriented nuclei, respectively. The results of the experiment are shown in Fig. 2. Curve 1 represents a Born-approximation calculation using Greenstein's method,¹⁸ in which the nucleus is assumed to be a uniformly charged ellipsoid of revolution with a quadrupole moment of 8.56×10^{-24} cm² and an rms charge radius of 6.58 fm. Curve 2 is the result obtained by Wright,¹⁹ assuming the charge distribution as previously described.

Greenstein treated the calculation in the Born approximation throughout, and absolute cross sections calculated in that fashion deviated markedly from our data. The theoretical cross sections were in general too small, and at diffraction minima they were a factor of 3 to 10 lower than the data. The Born approximation is known to be poor in the region of diffraction minima. In addition, the sharp-edged nuclear model necessary for Greenstein's calculations also drastically deepened the minima.

Wright obtained a reasonable preliminary fit to the absolute cross section (see Fig. 3) for randomly oriented nuclei, but his results for the alignment effect are only moderately better than those of Greenstein. One reason for the similarity is that both the authors are forced to use some version of Born approximation to calculate the change in cross section due to the nonspherical contribution to the nuclear potential. The method of phase shifts cannot be applied to such a problem, yet the Born approximation is clearly inadequate for Ho¹⁶⁵ for which $Ze^2/\hbar c = 0.5$.

Both theories do predict the general character of the effect. The maxima and minima of the theoretical curves and of the data occur at approximately the same energies. The data show a behavior periodic in the momentum transfer, with a period of about 0.54 fm⁻¹, one-half that of the monopole form factor. This is consistent with a monopole-quadrupole interference term, originally predicted by Downs, Ravenhall, and Yennie.²⁰ The interference term should show a form similar to the product $j_1(qR)j_2(qR)$,¹⁸ where j_1 and j_2 are the spherical Bessel functions which arise incoherently in the Born-approximation calculations for unoriented nuclei.

The alignment effect Δ should be proportional

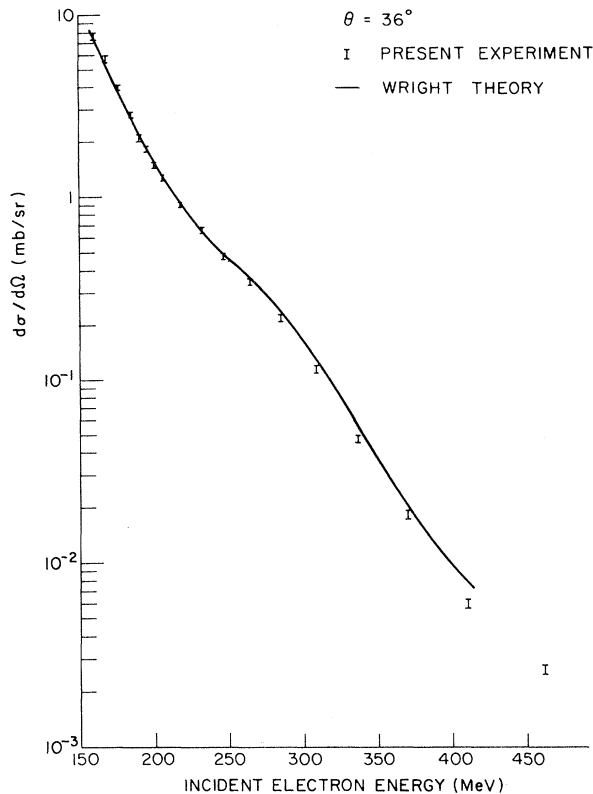


FIG. 3. Comparison of the experimental differential cross section for randomly oriented Ho^{165} nuclei with the theoretical calculation by Wright.

to the static quadrupole moment of the nucleus. However, if we allow the quadrupole moment to be reduced enough to improve the fit to Δ , the agreement with the random differential cross sections is lost. There are several weak points in the theories that may account for some of this inconsistency. In addition to the problems with the Born approximation, there is the fact that inelastic excitations must be included in the calculation because of the energy resolution of our experimental apparatus. These excitations are calculated only to first order, thereby omitting any inelastic interference effects. The inelastic excitations may contribute as much as 30% of the absolute cross section, making it difficult both to calculate and to measure the small alignment effect.

The models of the nuclear-charge distribution may be inadequate to describe Ho^{165} . Both Greenstein and Wright used models in which the quadrupole moment was ascribed to a deformity localized at the surface of the nucleus. It might be of interest to compute the effect of a distorted nuclear core on the predicted effect.

The development of a He^3 - He^4 dilution refriger-

ator²¹ with sufficient heat-removal capability should make it possible to perform similar experiments with other deformed nuclei of the rare-earth group. The process could then be extended to lighter nuclei in which the first excited states are high enough in energy to allow experimental resolution. It may be possible by this method to isolate the particular physical aspect of the problem that presently causes the disagreement between theory and experiment.

*Work supported in part by the U. S. Office of Naval Research under Contract No. Nonr 225(67) and by the National Science Foundation.

†Present address: Department of Physics, University of Virginia, Charlottesville, Va. 22901.

¹R. Hofstadter, *Nuclear and Nucleon Structure* (Benjamin, New York, 1963).

²J. Heisenberg, R. Hofstadter, J. S. McCarthy, I. Sick, B. C. Clark, R. Herman, and D. G. Ravenhall, *Phys. Rev. Lett.* **23**, 1402 (1969).

³B. Hahn, D. G. Ravenhall, and R. Hofstadter, *Phys. Rev.* **101**, 1131 (1956).

⁴R. S. Safrata, J. S. McCarthy, W. A. Little, M. R. Yearian, and R. Hofstadter, *Phys. Rev. Lett.* **18**, 667 (1967).

⁵N. P. Heydenburg and G. M. Temmer, *Phys. Rev.* **104**, 981 (1956).

⁶E. G. Fuller and E. Hayward, *Nucl. Phys.* **30**, 613 (1962).

⁷W. C. Koehler, J. W. Cable, M. K. Wilkenson, and E. O. Wollan, *Phys. Rev.* **151**, 414 (1966).

⁸O. V. Lounasmaa, *Phys. Rev.* **128**, 1136 (1962).

⁹R. Ratnalingham and J. B. Sousa, *Phys. Lett.* **30A**, 8 (1969).

¹⁰See, for example, H. A. Bethe and J. Ashkin, in *Experimental Nuclear Physics*, edited by E. Segre (Wiley, New York, 1953), Vol. 1, p. 254.

¹¹L. R. Suelzle and M. R. Yearian, in *Proceedings of the International Conference on Nucleon Structure at Stanford University, 1963*, edited by R. Hofstadter and L. I. Schiff (Stanford Univ. Press, Stanford, Calif., 1964), p. 360.

¹²R. Hofstadter, F. Bumiller, B. R. Chambers, and M. Croissiaux, in *Proceedings of the International Conference on Instrumentation for High Energy Physics, Berkeley, California, September 1960* (Interscience, New York, 1961), p. 310.

¹³See, for example, J. Loeb, *C. R. Acad. Sci.* **222**, 488 (1946); and J. L. Symonds, *Rep. Progr. Phys.* **18**, 116 (1955).

¹⁴A. Bohr and B. R. Mottelson, *Kgl. Dan. Vidensk. Selsk., Mat.-Fys. Medd.* **27**, No. 16 (1953).

¹⁵J. Kern, G. Mauron, and B. Michaud, *Helv. Phys. Acta* **41**, 1280 (1968).

¹⁶L. W. Mo and Y. S. Tsai, *Rev. Mod. Phys.* **41**, 205 (1969). Some omissions in formulas in this article were pointed out to us by G. Miller; corrected formulas may be found in G. Miller, thesis, Stanford Univer-

sity, 1970 (unpublished).

¹⁷L. E. Wright, Nucl. Phys. **A135**, 139 (1969).

¹⁸H. Greenstein, Phys. Rev. **144**, 902 (1966).

¹⁹L. E. Wright, private communication.

²⁰B. W. Downs, D. G. Ravenhall, and D. R. Yennie,

Phys. Rev. **106**, 1285 (1957).

²¹See, for example, O. E. Vilches and J. C. Wheatley, Phys. Lett. **24A**, 440 (1967); T. R. Fisher, D. Healey, D. Parks, S. Lazarus, J. McCarthy, and R. Whitney, Rev. Sci. Instrum. **41**, 684 (1970).

Cloud-Chamber Search for $\frac{1}{3}e$ and $\frac{2}{3}e$ Quarks in Air Showers*

W. E. Hazen

University of Michigan, Ann Arbor, Michigan 48104

(Received 29 January 1971)

A cloud chamber of horizontal area 0.2 m² is being used to observe the ionization by the particles in the vicinity of the center of air showers in the manner of McCusker. No particle tracks with ionization typical of charge $\frac{2}{3}e$ or $\frac{1}{3}e$ have been found in 3200 shower photographs taken with a trigger rate of about one per hour.

An experiment similar to that of McCusker¹ is being conducted to search for evidence of fractionally charged particles in cosmic-ray air showers by observing the ionization of tracks in a cloud chamber. The ionization is proportional to the square of the charge and is somewhat energy dependent in the relativistic realm.² The cloud chamber and photographic system are designed to produce resolved images of individual drops. Furthermore, the plus- and minus-ion columns are separated in order to give a measure of drop-to-ion ratio.³ Thus, the translation of images on the film to ionization in real space can be done quite accurately.

The upper 35 to 40 cm of the chamber is used to observe relatively long sections of tracks. The bottom of the chamber contains a $\frac{1}{2}$ -in. Al and a $\frac{1}{2}$ -in. Pb plate, which are intended primarily for a rough determination of electron energies.

The relative time of arrival of a particle that forms a track in the upper part of the chamber can be measured from the separation of the plus and minus ions. The clearing field (electric field before the trigger) is about 30 V/cm vertically downwards, and the separation field (field after the trigger) is about 6 V/cm horizontally to the right. Consequently, a pre-trigger particle track can be identified more easily than a post-trigger track. In both cases, the plus-minus ion separation gives a more sensitive measure of relative age than the width of an ion column, since the former is linear in time t (for a given electric field), whereas the latter varies only as $(t)^{1/2}$. The field between the plates is about 20 V/cm, vertical, dropping to about 3 V/cm when the trigger occurs.

The time sequence for tracks of trigger age is such that the "width" of an ion column (track width) is ~ 2 mm. The horizontal component of the plus-minus column separation is ~ 4 mm between centers in the upper part of the chamber, the vertical component ~ 1 mm. The plus-minus column "separation" is vertical and about 3 mm for tracks between the plates.

The compromises among image illumination, depth of focus, film grain, and image size (with the limitation of the available capacitor bank for the flash tubes) led to the choice of 70-mm film. The chamber is photographed in two contiguous 10-cm thick vertical sheets by a double stereo camera with shutters synchronized with flashes that illuminate one sheet at a time. The average magnification is 1/7.

Images of drops near the end windows are brighter than near the center partly because of a stronger drop illumination but mostly because of a smaller scattering angle. The lenses of each stereo pair were usually set at different f stops, one favoring tracks at the center, the other at the ends of the chamber.

The chamber is located in a top-floor room with a concrete and hollow-tile roof construction that averages about 10 cm in thickness, that is, nearly a radiation unit. The trigger is a local particle-density trigger with a rate of approximately one per hour. About half the triggers are due to showers whose axes hit within 8 m. In terms of energy of the initiating primary cosmic ray, about half the triggers are due to E from 2×10^{15} to 10^{16} eV, and the other half to $E > 10^{16}$ eV.

The films are scanned stereoscopically with $5 \times$ magnification by physics majors and physics